CHAPTER TWENTY EIGHT

Field Studies of Run-up on Dissipative Beaches

Christopher T. Carlson*, A.M. ASCE

Abstract

Field measurements of narrow-band incident wind waves and the resulting run-up were made photographically at two different natural sand beaches along San Francisco Bay. The run-up spectra derived from the field-measured time series show some energy at the incident-wave peak frequency, with the predominant run-up spectral energy concentrated in frequency bands below the incident-wave peak frequency. Observations of the swash time series recorded at both beaches indicate that the low-frequency run-up is generated on the beach face by the interaction between the run-up and backwash during the swash cycle.

Coherence analyses indicate that the offshore incident waves and run-up on the beach are not linearly correlated but that the run-up is correlated in the alongshore direction. The slopes of the log-log run-up spectra computed over the frequency band of the incident waves are all approximately -3. Statistical hypothesis tests were used to compare the empirical run-up cumulative distribution functions with both normal and Rayleigh distribution functions.

Introduction

The frequency band containing the dominant run-up spectral energy is generally not the same as the frequency band of the predominant incident-wave energy. For this reason, offshore wave statistics may not provide good estimates of the frequency distribution of wave energy expected at the shoreline or on the beach. A shift in the run-up spectral energy to frequencies lower than the predominant incident-wave frequencies has been observed for the run-up generated by a broadband incident-wave field. Field measurements of wave run-up reported in the open literature are very limited and most are by-products of edge wave or standing wave studies conducted on open ocean coasts where the incident-wave fields were usually swell dominated. The incident-wave/beach slope combinations generally produced highly reflective conditions, and the low-frequency (LF) run-up observed or measured during the experiments was attributed to modulation of the run-up by standing waves or edge waves present near the shoreline. No measurements have been reported for the run-up generated on a dissipative beach by narrow-band wind waves only.

*Oceanographer, Sohio Petroleum Co., One Lincoln Centre, 5400 LBJ Freeway, Suite 1200-LB 25, Dallas, TX 75240

LF swell-derived components in the run-up spectrum can often obscure other low-frequency contributions to the run-up that are developed on the beach by the higher-frequency wind waves in the incident-wave field.

Objective

The objective of this study was to measure LF run-up generated on the beach face by the interaction between the run-up and backwash during the swash cycle. The experiments were designed to measure run-up on dissipative beaches exposed only to relatively high-frequency, narrow-band wind waves that broke near the shoreline by plunging. These conditions generally minimize or eliminate standing wave, edge wave, or very-low-frequency surf-beat components from the run-up that are derived from the swell component in an incident-wave field.

Field Experiments

On 14 December 1977, incident wave and run-up measurements were made at the R.W. Crown Memorial State Beach on the eastern shore of San Francisco Bay (western shore of Alameda Island); similar measurements were subsequently made along the western shore of the bay on 14 May 1982 at Coyote Point Beach (Figure 1). Two separate field sites were selected to provide independent data sets for different beach slopes exposed to different incident wind-wave fields. It was necessary to avoid reflective beach conditions for which nonlinear perturbation of the incident-wave field by edge or standing waves might affect the frequency distribution of the run-up on the beach face. The field measurements were therefore conducted for dissipative beach conditions.

Beach reflectivity and inshore resonance may be characterized by the surf scaling parameter, $\epsilon = a\omega^2/g \tan^2\beta$, where a is the incident wave amplitude, ω the radian wave frequency and β the beach slope. Reflective, dissipative and highly dissipative beach conditions are characterized by respective ϵ values of less than about 2.5, greater than 2.5 and greater than 33. The moderately dissipative regime studied here, is identified by a relatively narrow surf zone, plunging breakers, and strong run-up. Beach reflectivity conditions for these field experiments yielded ideal ϵ values of 6 (Alameda) and 19 (Coyote Point).

Alameda Beach

The Alameda Beach was composed of fine- to medium-grained silica sand and was openly exposed to westerly and southwesterly winds (Figure 1). The angle of wave approach was nearly normal to the shoreline as wind speeds increased from 3 m/s to over 5 m/s from 170

degrees true. A single breaker zone was located approximately 3 m (9.8 ft) from the shoreline, and all waves broke by plunging. The measurements were made during the peak of the afternoon high tide.

A 16-mm Bolex movie camera was used to simultaneously record time series of the offshore incident waves and the run-up on the beach face along a single line of 25 aluminum reference stakes. The reference stakes were positioned in a linear transect normal to the shoreline extending about 14 m (45.9 ft) in the offshore direction (Figure 2) and were used to calibrate the time series of the incident waves and run-up measurements. The camera was positioned on a 1-m (3.3 ft) high bluff just shoreward of the reference stake array.

Transit and level field survey methods and direct tape measurements were used to establish the position and elevation of the reference stakes relative to a fixed datum stake and the camera. The elevations were surveyed accurate to 0.3 cm (0.01 ft), as were the horizontal distances. Reference surveys that included offshore profiles were made both before and after the experiment and confirmed that no measurable change occurred in the offshore profile during the experiment. Agreement between the measured and computed heights and positions of the reference stakes was better than 1 cm (0.03 ft) in all cases. The Alameda beach had a nearly linear slope of approximately 0.11 (6.2°), becoming nearly horizontal about 12 m (39.4 ft) offshore.

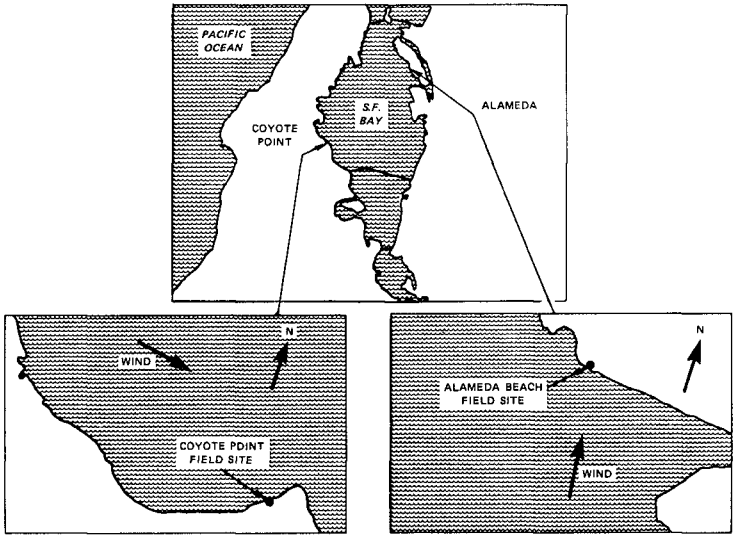

FIGURE 1 MAP SHOWING THE LOCATION OF THE ALAMEDA AND COYOTE POINT FIELD SITES AND THE PREDOMINANT WIND DIRECTIONS THAT PREVAILED DURING EXPERIMENTS

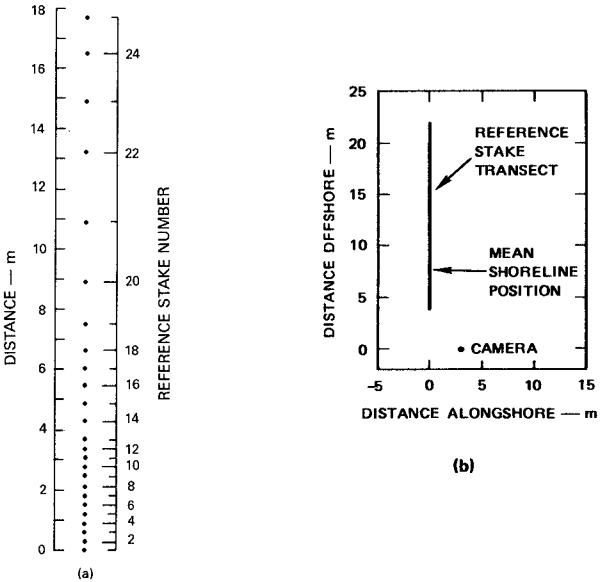

FIGURE 2 PLAN VIEWS OF ALAMEDA BEACH REFERENCE STAKE ARRAY SHOWING (a) REFERENCE STAKE NUMBERS AND SPACING BETWEEN STAKES AND (b) LOCATION OF CAMERA RELATIVE TO REFERENCE STAKE TRANSECT AND APPROXIMATE SHORELINE POSITION.

Coyote Point Beach

The beach at Coyote Point was openly exposed to northerly and northwesterly wind waves (Figure 1) and the beach was composed of very small gravel and coarse sand. The beach slope was nearly constant in both the alongshore and offshore directions and formed a low-energy dissipative system with the incident-wave conditions present during the experiment.

The movie camera used for the Alameda field experiment was also used for the Coyote Point measurements. A two-dimensional grid of 80 wooden reference stakes arranged in 10 shore-normal transects provided the datum control for the Coyote Point experiment (Figure 3). Level and transit field survey techniques described for the Alameda measurements were used to establish datum control with the same accuracies. Three long transects and seven shorter ones crossed the beach face and extended offshore. The stakes located on the beach face were spaced closer together than those offshore to increase the available resolution for the run-up measurements. Figure 4 shows the orientation of the reference stake array relative to the camera, which is positioned at the origin of the plot. Also shown is a triangular array of three stakes located well seaward of the breaker zone and used for definition of the offshore incident-wave field.

To maintain continuity of the mean water level during the experiment, time series were recorded during the peak of the high tide. The winds were quite strong (about 8 m/s) and were nearly constant in their direction (250° true) throughout the experimental period. The waves were nearly normal in incidence to the beach at the location of the reference stake array and plunging breakers were observed throughout the experiment. No visible signs of edge wave activity, such as beach cusps or regular alongshore spatial modulation of the run-up, were observed at any time during the experiment. Only one breaker zone was present near the shoreline.

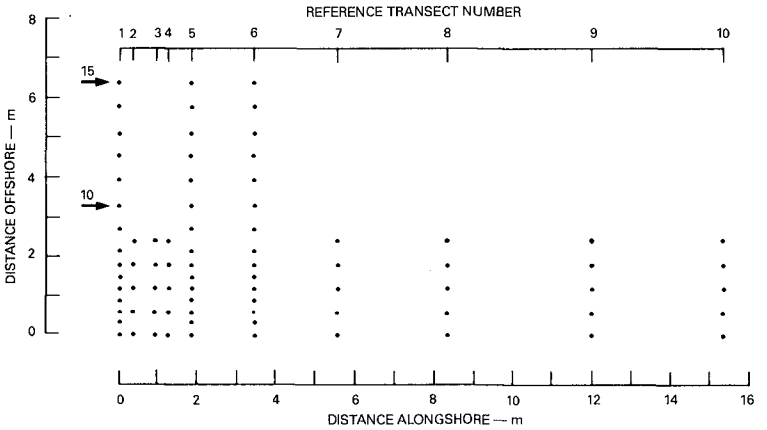

FIGURE 3 PLAN VIEW OF THE TWO-DIMENSIONAL ARRAY OF REFERENCE STAKES USED FOR THE COYOTE POINT RUN-UP FIELD EXPERIMENT

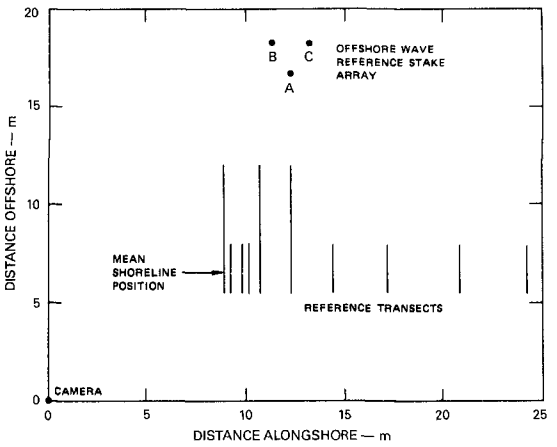

FIGURE 4 PLAN VIEW SHOWING LOCATION OF THE CAMERA RELATIVE TO REFERENCE STAKE TRANSECTS AND OFFSHORE INCIDENT-WAVE REFERENCE STAKE ARRAY

Data Analysis

Time series of the incident waves were derived from the 16-mm photographic record by digitizing the amplitude fluctuations of the waves where they passed the offshore reference stakes. Similarly, the run-up time series were developed from the movie record by digitizing the position of the leading edge of the run-up on the beach face.

The movie frames were digitized manually using an electronic photodigitizer. The oblique photographic image was projected onto a Tektronix 4956 Graphics Tablet connected to a Tektronix 4052 terminal; an electronic pad with crosshairs was used to digitize the photograph. The digitized points were stored on cassette tape and subsequently transferred from the Tektronix terminal to a DEC VAX 11-782 computer for processing and analysis.

The leading edge of the run-up on the beach face was digitized in the photographs along the reference stake transect. It was relatively easy to identify the position of the leading edge of the run-up in the photographs due to the presence of seafoam on the beach. The seafoam provided an effective tracer of run-up in the photographs since it closely followed the moving shoreline. In addition, the flow pattern around other inundated reference stakes was readily evident and proved helpful in verifying the continuity of the swash layer on the beach face. The run-up time series were calibrated into physical units directly from the photographs by using the surveyed reference stake positions. The positions of the reference stakes computed from the photographs agreed to within 2.5 cm (0.08 ft) of the measured positions.

The incident-wave amplitude time series were developed by digitizing the fluctuating water surface at the stakes. As with the digitized run-up time series, the product of digitizing was a digital time series of oblique photo coordinates in arbitrary digitizer units. No calibrations were available for the middle of the unmarked offshore reference stakes, near the mean water level, where the waves passed the stakes, thus precluding direct calibration. Photogrammetric analysis techniques were used to calibrate the incident-wave time series. The equivalent vertical photograph method of analysis (2,8,13) was used to compute the real ground coordinates of the offshore reference stakes and to calibrate the wave amplitude time series.

All incident-wave and run-up time series data computed from the Alameda and Coyote Point photographs were processed identically using standard digital time series analysis techniques. The results of four primary categories of processing are presented; spectral analysis, coherence and phase analysis, computation of spectral slopes, and statistical hypothesis testing on the empirical cumulative distribution functions (CDFs). Both chi-square (X^2) and Kolmogorov-Smirnov (KS) goodness-of-fit tests were used to compare the empirical CDFs to both normal and Rayleigh distributions.

Results

Alameda Beach

Due to preset camera exposure rates, the raw time series data were recorded at 10.66 Hz and were subsequently down-sampled to 5.33 Hz during the digitizing process. A total of 1024 time series points were processed for both the incident waves and run-up, representing approximately 192 s of data. A 128-point FFT window was used, which corresponded to a 24-s time series segment, giving a Nyquist frequency of 2.67 Hz and a spectral resolution of 0.042 Hz. The use of a 50% spectral overlap with the power-normalized Hanning window produced 26 equivalent degrees of freedom for the spectral estimates (12).

Figure 5 shows the power spectral density (PSD) computed for (a) the incident waves recorded at reference stake 19 (Figure 2) and (b) the run-up recorded on the beach face plotted against frequency in Hertz. The predominance of LF run-up spectral energy at frequencies not containing high energy densities in the incident-wave spectrum is striking. The absolute magnitude of the power in the run-up spectrum is greater than that of the incident-wave spectrum. This is because the component of swash motion measured parallel to the plane of the beach face was recorded in these experiments and is reported here. If the vertical component of run-up had been computed, the absolute magnitude of the run-up spectral values would have been smaller, but the frequency distribution of the energy would remain the same.

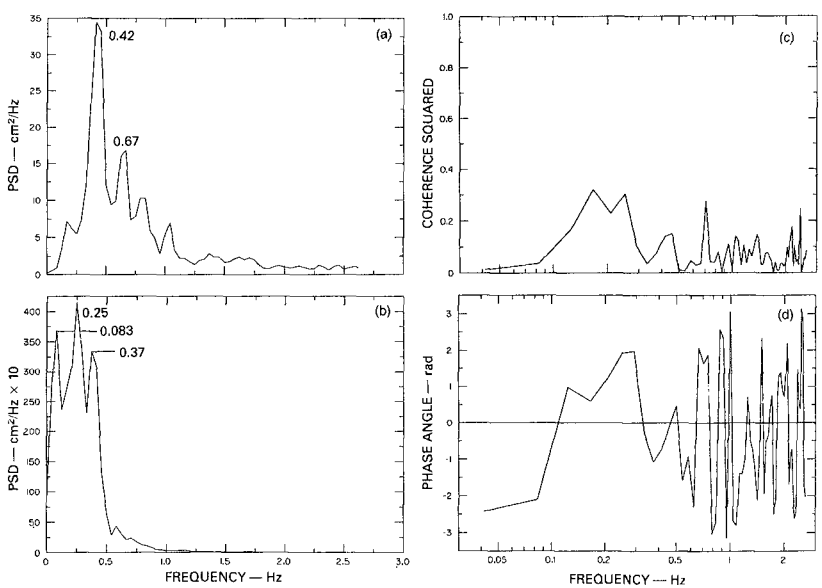

FIGURE 5 ALAMEDA BEACH (a) INCIDENT-WAVE AND (b) RUN-UP SPECTRA WITH THE ASSOCIATED (c) COHERENCE AND (d) PHASE.

The frequencies of the dominant peaks in the spectra are indicated on the plots. The frequency resolution is 0.042 Hz, and the absolute position of any given spectral peak with respect to frequency may vary by a single resolution cell in either direction. The 0.42-Hz peak in the wave spectrum can be assumed to match the 0.37-Hz peak in the run-up spectrum. Guza and Thornton (6) also report the presence of a peak in the run-up spectrum at the incident-wave frequency for run-up measured on steep beaches with narrow surf zones. The wave spectrum is virtually devoid of energy at the 0.083- and 0.25-Hz frequencies containing the majority of the energy in the run-up spectrum. Conversely, the run-up spectrum does not exhibit energy at frequencies higher than about 0.5 Hz, whereas significant wave energy is present at frequencies greater than 0.5 Hz.

The incident-wave and run-up spectra were recomputed using a log-log format. Spectral slopes were then computed for these spectra over the so-called saturation frequency band of the incident wind waves by using a linear least-squares regression analysis. The slope computed for the wave spectrum is -1.9 and for the run-up spectrum is -3.2. The saturation band was defined over the frequency band of the incident wind waves that broke near the shore (6,7). Since the data recorded for the Alameda and Coyote Point field experiments contained only wind-wave characteristics, the saturation region of the spectrum was defined as all frequencies equal to and greater than the incident-wave peak frequency.

Figure 5 also shows the (c) coherence squared and (d) phase computed between the incident-wave and run-up time series. Following Bendat and Piersol (4), the 95% confidence limits are given in the Appendix (Table A-1) as a function of coherence. At the 5% level of significance ($\alpha = 0.05$), the hypothesis that $\gamma_{xy} = 0$ results in an acceptance region for the variable equal to 0.19. The coherence is generally low across the entire frequency band, and the phase is random, indicating that the waves and run-up are not linearly correlated. This lack of linear coherence between the offshore incident waves and the run-up on the beach face is not surprising and has been observed by others. The coherence between the time series was completed both with and without compensation for the spatial separation between the measurement locations.

The CDFs were computed for the Alameda incident waves and run-up. Two different data formats were used in comparing the empirical CDFs with normal and Rayleigh CDFs. For hypothesis testing of the measured data with respect to the model normal distribution, the incident-wave and run-up amplitude time series were converted to time series of standard deviations using: $x(t) = (x(t) - E[x(t)])/\sigma_x$ where E[] is the expected value and σ_x is the standard deviation. Prior to computing the Rayleigh CDFs, the run-up and incident-wave time series were redefined for the comparisons using: $x(t) = x^2(t)/\langle x^2(t)\rangle$.

With the exception of the Rayleigh distribution for the waves, the empirical distributions provide a very close fit to both the normal and Rayleigh distributions and it might be tempting to conclude that

both distributions provide a good fit to the data. A KS goodness-of-fit test was used to quantify the agreement between the empirical, normal, and Rayleigh distributions. Only the incident-wave and normal CDFs appeared to be statistically the same with respect to the KS test statistic. That is, the two CDFs were not statistically different based on the KS test statistic. It should be emphasized here that these statistical tests do not indicate the distribution to which the empirical data conform; rather, the tests identify model statistical distributions from which the empirical distribution is not different. It is also possible that some other statistical distribution, not tested here, may fit the empirical run-up and incident-wave distributions.

Coyote Point Beach

The Coyote Point reference stakes were numbered consecutively in the offshore direction from 1 to 15 in transect 1 (Figure 3). The incident waves were measured at four offshore locations, which included reference stakes 10 and 15 in transect 1 and points A and B in the offshore reference stake triangle shown in Figure 4. The waves were steepening or just beginning to break as they reached stake 15; the largest waves broke by plunging just seaward of stake 15, while the smaller waves broke by plunging just shoreward of stake 15. The waves measured at stake 10 were actually bores moving shoreward toward the beach. The run-up was measured along transects 1, 3, 5, and 6 spanning an alongshore distance of approximately 3.5 m (11.5 ft).

The Coyote Point series data were recorded at 14 Hz and were downsampled to 3.5 Hz during digitizing. All eight time series were time-registered. Spectral analysis of these data was accomplished using 36-s, 128-point FFTs, producing a spectral resolution of 0.027 Hz and a Nyquist frequency of 1.75 Hz. The 50% spectral overlap, Hanning window, and other processing techniques described for the Alameda data were used to produce the spectra with 23 equivalent degrees of freedom.

The incident-wave spectra computed for the data recorded at offshore stakes A and B and along transect 1 at stakes 10 and 15 are shown in Figure 6. The spectral peak frequencies between all four of the spectra agree to within 1 frequency resolution cell. The spectra measured at all four locations are uniformly narrow-band, with one primary frequency. Virtually no LF energy is observed in any of the incident-wave spectra measured either well offshore at stakes A and B or nearer the shoreline at stakes 10 and 15.

A net decrease in wave height was observed across the reference stakes moving shoreward in order B-A-15-10. Respective rms wave heights of 10.0, 9.7, 8.6 and 5.1 cm (0.33, 0.32, 0.28, 0.17 ft) were computed for these locations both directly from the time series variance and by integration of the spectra from zero to the Nyquist frequency. Agreement between the two methods was uniformly better than 1%. Some transfer of spectral energy from lower to higher frequencies is observed in the spectra computed for stakes 10 and 15.

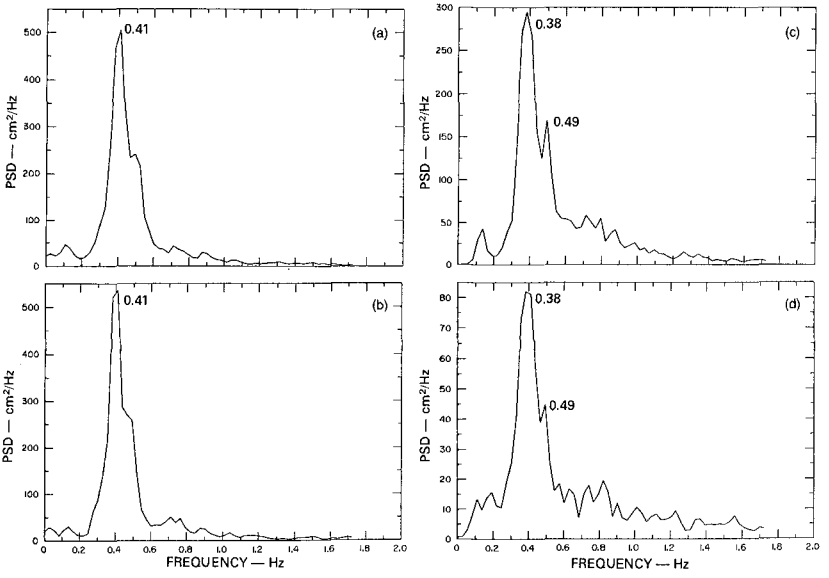

FIGURE 6 COYOTE POINT INCIDENT-WAVE SPECTRA MEASURED AT REFERENCE STAKES (a) B, (b) A, (c) 15 AND (d) 10

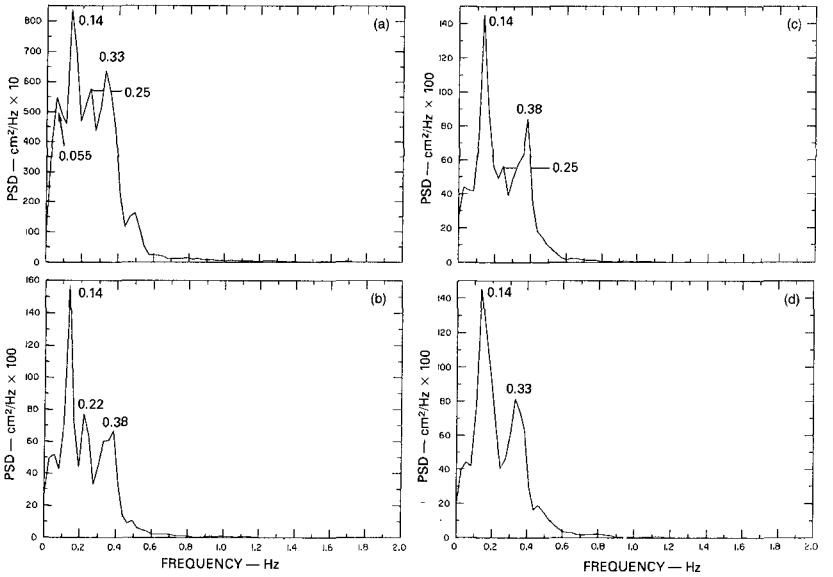

FIGURE 7 COYOTE POINT RUN-UP SPECTRA MEASURED ALONG REFERENCE TRANSECTS (a) 1, (b) 3, (c) 5 AND (d) 6

The run-up spectra measured at reference transects 1, 3, 5 and 6 are shown in Figure 7. The predominance of the LF energy in each run-up spectrum is the most noteworthy feature. The spectral peak frequency of the incident waves was approximately 0.38 Hz and although each of the measured run-up spectra show some energy at this frequency, the predominant run-up energy is located at much lower frequencies as observed for the Alameda Beach data. The 0.14 Hz spectral peak is observed in all of the run-up spectra measured at Coyote Point. A peak at 0.22 to 0.25 Hz (1 resolution cell apart) is observed in the run-up spectra measured at transects 1, 3 and 5.

The predominant run-up and backwash motions at frequencies 0.14 and 0.38 Hz were readily observed along all of the transects analyzed here. Although the frequency resolution of all four run-up spectra is identical, there appears to be a loss of fine structure detail in the spectra moving from transect 1 to transect 6. This is attributed to the increased distance between the measurement point and the camera location (Figure 4), coupled with the photographic resolution of the small 16-mm film. During analysis, it was increasingly difficult to observe the fine structure of the swash motions as transects located further from the camera were analyzed. For this reason, the continuum of energy located in frequency bands surrounding the dominant 0.14- and 0.38-Hz peaks in the run-up spectra recorded at transects 3, 5 and 6 is not as pronounced as in the spectrum recorded at transect 1. The basic shape of the energy continuum surrounding the 0.14-Hz spectral peak is conserved in the spectra measured at transects 1, 3 and 5 as is the total energy in the spectra. The rms run-up computed in the plane of the beach face at transects 1, 3, 5 and 6 was respectively 50.3, 55.2, 53.4 and 55.4 cm (1.65, 1.81, 1.75, 1.82 ft).

The spectral slopes were also computed over the saturated frequency band of the breaking incident wind waves for the run-up and incident-wave data recorded at Coyote Point . The slopes given in Table 1 compare favorably with the slopes computed for the Alameda data and show good agreement with slopes reported recently by others (6,7) for measurements made at beaches exposed to both swell and wind waves simultaneously. The slopes of the incident-wave spectra decrease in the shoreward direction. This appears to be explained by the transfer of energy in the spectrum from lower to higher frequencies as the waves shoal and break.

Table 1

COYOTE POINT SPECTRAL SLOPES

Run-up Location	Slope	Wave Location	Slope
1	-2.8	B	-3.1
3	-3.0	A	-3.0
5	-2.9	15	-2.7
6	-3.1	10	-1.8

To estimate the onshore-to-offshore correlation between the run-up and the incident waves, the coherence and phase were computed between the run-up measured at reference transect 1 and the incident waves measured at reference stakes B, 15 and 10. Figure 8(a) shows the coherence squared and the phase computed between the run-up and the waves measured at offshore stake 15. The acceptance region for $\gamma_{xy} = 0$ at the 95% confidence interval is 0.21. These results are typical of those computed between measurements made at the other locations. In each case, the correlation between the incident waves and the run-up is low.

The alongshore correlation in the run-up was also examined by computing the coherence and phase between all combinations of the run-up time series measured at transects 1, 3, 5 and 6. The coherence and phase between the run-up measured at transect 1 and 3 shown in Figure 8(b) is representative of all transects. Phase in the run-up correlations is generally random above 0.4 Hz, and coherence is low. Coherence squared was generally high between all four run-up transects across the lower frequency bands containing the predominant run-up spectral energy, reaching a maximum of approximately 0.8. The alongshore correlation in the run-up tends to decrease, however, with increasing separation between measurement points. Across all transects, the coherence remains consistently high near 0.14 and 0.38 Hz, the frequencies of the dominant peaks in the run-up spectra. The phase is nearly constant and is approximately zero in the band of frequencies less than 0.3 Hz, where the coherence is high, indicating that the time series are in phase.

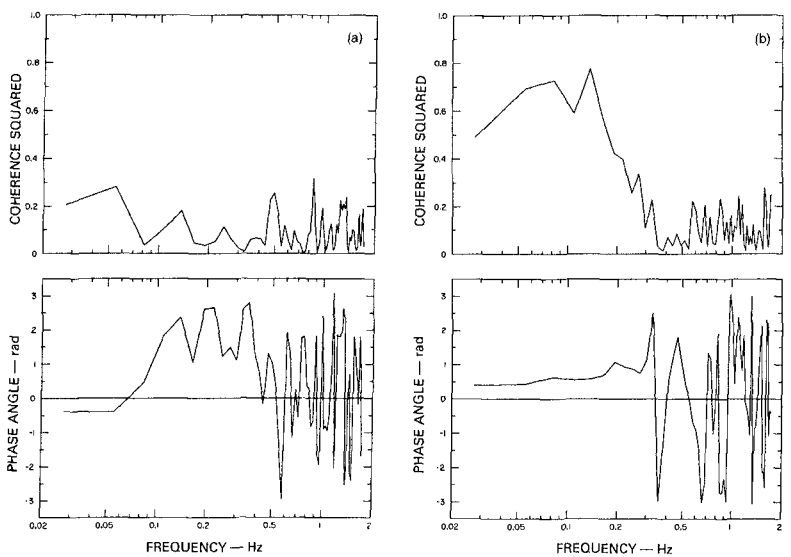

FIGURE 8 COYOTE POINT COHERENCE AND PHASE BETWEEN THE RUN-UP ALONG TRANSECT 1 AND THE (a) INCIDENT WAVES AT STAKE 15 AND (b) THE RUN-UP ALONG TRANSECT 3

The CDFs computed for the run-up measured at transects 1, 3, 5 and 6 and for the incident waves measured at stake A were compared to model normal and Rayleigh distributions using X^2 and KS statistical hypothesis tests. In each instance, the fit between the normal and data-derived run-up CDFs is very close. The KS tests results show that the null hypothesis cannot be rejected at the 95% confidence interval in any of the tests, and thus a normal distribution is not statistically different from the distribution of the Coyote Point run-up data for all four transects reported here. The observed value of the X^2 statistic was less than the expected value in each case, and thus, the X^2 test also confirms that the Coyote Point run-up data are not different from a normal distribution at the 95% confidence interval.

When tested against a Rayleigh distribution, the tests show that the Coyote Point run-up is statistically different from a Rayleigh distribution at the 95% confidence interval. The distribution of wave heights measured at A is statistically different from both the Rayleigh and normal distributions at the 95% confidence interval but is not different from a normal distribution at 99%.

Discussion

Two different field sites were selected, each with similar yet statistically different incident-wave and beach slope conditions, and in both cases low-frequency wave run-up was observed with similar characteristics. A small percentage of run-up energy was observed at the incident-wave peak frequency, but the largest percentage of the run-up energy was located at frequencies that were significantly lower. The fact that some run-up spectral energy is located at the predominant incident-wave frequency indicates that although wave-breaking by plunging is highly nonlinear, there is some memory involved whereby incident-wave frequency information is transferred to the run-up. The mechanism for this transfer may be the collision between the seaward-moving backwash and the shoreward-moving incident bore.

Observations of the run-up made during the field experiments revealed a typical swash-cycle scenario. A wave broke by plunging in the shallow water near the shoreline forming a bore that traveled a very short distance before running up the beach. Before this first wave reached the run-up limit and began its backwash, a second or even third wave plunged and surged up the beach face over the top of the moving layer of water created by the first wave(s). The backwash generated by the combination of these earlier waves would often attenuate the run-up of the subsequent wave, producing a modulation of the swash. Because a spectrum of incident-wave frequencies was present, albeit a narrow one, the relative timing between the run-up and backwash was not constant, thus creating the spectrum of low run-up frequencies.

The red-shift observed in run-up spectra may be caused by different mechanisms. The beach can behave as a low-pass filter to

the incident waves when exposed to a broadband spectrum of incident-wave energy. When exposed to both long swell waves and shorter wind waves, the longer waves produce the dominant, large run-up excursions, and the run-up generated by the shorter waves becomes embedded in the long-wave run-up. As a result, the run-up spectrum shows a prominent peak at the long-wave frequency, as well as at other frequencies.

Unlike the run-up field data reported in the open literature, however, the Alameda and Coyote Point run-up measurements were made for wind-wave conditions exclusively. The Alameda and Coyote Point incident-wave fields were narrow-band in frequency and contained only one predominant wind-wave component. The peak in the run-up spectrum coincident with the incident-wave peak frequency was not produced by long waves masking the run-up generated by shorter waves. Instead, the incident wind waves produced components in the run-up at their characteristic frequency and at lower frequencies through the interaction of the run-up and backwash during the swash cycle. If the beach were simply acting as a low-pass filter to the incident waves, the run-up spectral energy would be observed primarily at the wind-wave frequency only. There was no broadband distribution of incident-wave energy to be low-passed by the beach, but instead only one predominant forcing frequency.

No regular alongshore modulation of the run-up was observed at any time during the field experiments. The mean shoreline remained straight, and no edge wave derived cusps or regularly spaced deposits of seafoam or debris were observed along the shore. The time series of the run-up measured at transects 1, 3, 5 and 6 all showed approximately the same mean value. Thus, no quantitative alongshore variability of the mean run-up was observed over the 3.5-m (11.5 ft) distance between transects 1 and 6.

Huntley et al. (7) proposed a universal form for swash spectra. They observed an f^{-4} frequency dependence over the saturated portion of the run-up spectrum corresponding to the wind-wave band. Thornton (10) and Guza and Thornton (6) reported swash measurements for which an f^{-3} frequency dependence was observed. While a -3 slope was measured for the Alameda and Coyote Point run-up spectra, these data do not identify whether the same mechanisms produce both the -3 and -4 spectral slopes. These data do, however, support the idea of a saturated run-up spectrum.

Both normal and Rayleigh distributions appear to provide reasonable models for the run-up amplitude distribution. Webber and Bullock (11) indicate laboratory measured run-up was best described by a normal distribution. Battjes (3) suggests that run-up is more appropriately modeled using a Rayleigh distribution based on an assumed Rayleigh distribution for the incident-wave heights and squared wave periods. Sawaragi et al. (9) used a Weibull distribution in their run-up distribution model and Ahrens (1) assumed a Rayleigh distribution for the run-up in his proposed method for predicting the run-up due to irregular waves. Formal statistical hypothesis test

results are often not reported in the open literature for comparisons between empirical data and a chosen model probability distribution. The agreement may not be acceptable quantitatively based on formal hypothesis tests. If the run-up distribution model proposed for use in a predictive capacity does not match the field conditions, the accuracy of the prediction may not be acceptable.

Conclusions

Field measurements of narrow-band, incident wind waves and the resulting run-up on the beach face were made at two different natural beaches. The run-up spectra measured at both beaches show LF energy concentrated at frequencies much lower than the frequency band of the predominant incident waves. No LF energy was observed in any of the incident-wave spectra measured either offshore or near the shoreline. No continuous offshore-to-onshore red-shifting of spectral energy was observed. Photographic observations of the swash cycle on the beach face indicate that the interaction between the run-up and the backwash appears to be the source of the low-frequency energy.

Coherence between the incident waves and the run-up is very low across the surf zone. Although some run-up spectral energy is present at the dominant incident-wave frequency, the coherence level in this frequency band is not statistically significant. Some incident-wave information appears to be transmitted to the run-up, but linear coherence estimates do not identify the mechanism.

An equilibrium region of the run-up spectrum appears to exist over the frequency band of the incident waves. Run-up spectra measured during both field experiments show consistent -3 slopes over the frequency band defined by frequencies greater than or equal to the incident-wave peak frequency.

The CDF computed for the Coyote Point run-up amplitude data is not statistically different from a standard (0,1) normal distribution. The Alameda run-up was statistically different from both normal and Rayleigh distributions, although qualitatively the data were more nearly normally distributed.

Acknowledgements

This work represents a portion of the author's Ph.D. dissertation research (5) conducted at the University of California, Berkeley, CA (UCB). The writer thanks Professors R.L. Wiegel and J.R. Paulling of UCB and Professor J.L. Hammack of the University of Florida for their advice and suggestions during this study. A special thanks to Dr. J.W. Maresca, Jr. of Vista Research, Inc. and Dr. E. Seibel of San Francisco State University, for their help during the field experiments. This study was completed with the generous support of SRI International, Menlo Park, CA and the Department of Hydraulic and Coastal Engineering at UCB. The author thanks Lynnett Doeden for typing the text and the Sohio Petroleum Company for supporting the preparation of this manuscript.

References

1. Ahrens, J., "Prediction of Irregular Wave Run-up," Coastal Engineering Technical Aid No. 77-2, U.S. Army, Coastal Engineering Res. Center, Fort Belvoir, VA, (1977).
2. American Society of Photogrammetry, Manual of Photogrammetry, 3rd Ed., Washington, DC, (1966).
3. Battjes, J.A., "Run-up Distributions of Waves Breaking on Slopes," J. Waterways, Harbors and Coastal Engineering Div., ASCE, No. WW1, pp 91-114, (1971).
4. Bendat, J.S. and A.G. Piersol, Random Data: Analysis and Measurement Procedures, (Wiley - Interscience, New York, NY 1971).
5. Carlson, C.T., "Field Studies of Run-up Generated by Wind Waves on Dissipative Beaches," Ph.D. Dissertation, Univ. of California, Berkeley, CA, (1983).
6. Guza, R.T. and E.B. Thornton, "Swash Oscillations on a Natural Beach," J. Geophys. Res., Vol. 87, No. C1, pp 483-491, (1982).
7. Huntley, D.A., R.T. Guza, and A.J. Bowen, "A Universal Form for Shoreline Run-up Spectra?," J. Geophys, Res., Vol. 82, No. 18, pp 2577-2581, (1977).
8. Maresca, J.W., Jr. and E. Seibel, "Terrestrial Photogrammetric Measurements of Breaking Waves and Longshore Currents in the Nearshore Zone," Proc. Fifteenth Coastal Engineering Conf., ASCE, Honolulu, HI, pp 681-900, (1976).
9. Sawaragi, T., K. Iwata and A. Morino, "Wave Run-up Height on Gentle Slopes," Coastal Engineering in Japan, 20, pp 83-94, (1977).
10. Thornton, E.B., "Energetics of Breaking Waves Within the Surf Zone," J. Geophys. Res., Vol. 84, No. C8, pp 4931-4938, (1979).
11. Webber, N.B. and G.N. Bullock, "A Model Study of the Distribution of Run-up of Wind-Generated Waves on Sloping Sea Walls," Proc. Eleventh Coastal Engineering Conf., ASCE, London, England, pp 870-887, (1968).
12. Welch, P.D., "The Use of Fast Fourier Transform for Estimation of Power Spectra: A Method Based on Time Averaging Over Short Modified Peridograms," IEEE Trans. Audio and Electroacoust., Vol. AU-15, pp 70-73, (1967).
13. Wolf, P.R., Elements of Photogrammetry, (McGraw-Hill, Inc., 1974).

Appendix

Table A-1

THE 95% CONFIDENCE LIMITS FOR $\gamma^2(f)$ WHEN DF = 26

$\gamma^2(f)$	0.4	0.5	0.6	0.7	0.8	0.9
Upper limit	0.64	0.72	0.78	0.84	0.90	0.95
Lower limit	0.087	0.17	0.28	0.42	0.58	0.78

DF = Number of degrees of freedom